

Kochi Chapter

Indian Geotechnical Conference

IGC 2022

15<sup>th</sup> – 17<sup>th</sup> December, 2022, Kochi

# A Numerical Study on the Abutment-Backfill System Subjected to Lateral Loading

Aritra Bagchi<sup>1</sup> and Prishati Raychowdhury<sup>2</sup>

<sup>1</sup> Department of Civil Engineering, Indian Institute of Technology, Kanpur, India, 208016

<sup>2</sup> Department of Civil Engineering, Indian Institute of Technology, Kanpur, India, 208016

**Abstract.** The abutment-backfill system plays an important role in transferring laterally generated forces from the bridge deck to the foundations on either end of the bridge. The soil used as the backfill material dictates the behaviour of the abutment-backfill system by mobilizing the forces in the form of stress. In a seat-type abutment, the in-plane lateral resistance is provided both by backfill and underneath piles, but the out-of-plane movement is mainly restricted by piles. It is necessary to study the behaviour of the abutment-backfill system under lateral loading. In the present study, a continuum 2D abutment-backfill-pile model is developed in OpenSees conforming to the site conditions of the Rohtak Railway Bridge project. Initially, a monotonic and cyclic pushover analysis is carried out to estimate the monotonic and cyclic capacity in terms of load-displacement curves. Two types of lateral loading conditions are chosen such as monotonic loading and sinusoidal loading. The global level behaviour at the critical positions is estimated to get an insight into the response characteristics of the system.

**Keywords:** Continuum, Monotonic, Pushover, Sinusoidal.

## 1 Introduction

With the urbanization and increase in the population, the need for public transport such as railway is rapidly growing nowadays. The importance of railway bridges cannot be neglected due to the high land acquisition cost and the necessity for shortest routes. During the operating time of the railway bridge, various forms of load and their combination are expected to occur at both superstructure and substructure levels. The direction and duration are the two main characteristics of the incoming load. Of them, direction refers to mainly vertical, transversal and longitudinal types of load while duration signifies temporary or permanent in nature. According to RDSO Bridge Rule, the sub-structure such as the abutment and pier consisting of sliding or elastomeric bearings should be designed for a maximum of 50% and 40% of the net longitudinal load respectively. Therefore, it can be expected that a considerable amount of static and dynamic longitudinal load will get transferred to the end support system from the bridge deck and eventually get resisted by the abutment foundation-backfill system. From the geotechnical aspect, both the backfill material and the foundation soil play a major role in controlling the performance of the end substructures through a complex soil-structure interaction mechanism.

Small and large-scale model tests along the numerical simulation of the abutment foundation-backfill system were conducted by several researchers in the past to capture

the response against static and dynamic loadings. A full-scale abutment model with granular and cohesive backfill was set up which was further subjected to static (Wilson and Elgamal 2010) and cyclic loading (Stewart et al. 2007; Lemnitzer et al. 2009). Besides, extensive numerical studies were carried out to explore the performance of the abutment-backfill in terms of lateral resistance under the presence of a variety of standard backfill soils and heights of the wall. Ellis and Springman (2001) prepared a reduced scale geotechnical centrifuge model of abutment-pile backfill on a soft clay layer overlying a granular substratum to investigate lateral soil-structure interaction effects considering the placement of the retained fill and associated deformation of the underlying soil. They further validated the results via a detailed finite element model simulating the centrifuge tests. Dicleli (2005) created a structural model of a typical integral bridge including the nonlinearity of the abutment-backfill system along with the piles and scrutinized the outcomes of having different geometric, structural, and geotechnical parameters on the performance of the abutment-backfill system under positive thermal variations. Argyroudis et al. (2013) simulated a seat-type abutment in a continuum domain using Plaxis 2D and side by side built up a non-linear bridge abutment spring model in SAP 2000 using the validated p-y curves of Plaxis. The models were analyzed for the collision force applied at the top of the abutment wall generalized it as a static force in one case and dynamic force history in the other. Argyroudis et al. (2013) established fragility curves for the cantilever bridge abutments lying on surface foundation under seismic shaking and investigated the effect of different parameters such as properties of foundation soil and backfill soil on the overall performance of the backfill-abutment numerically via Plaxis 2D.

Therefore, it is essential to accomplish an extensive numerical study focusing on the global level behaviour of the abutment-backfill system subjected to different forms of lateral loadings. In the present study, a continuum-based two-dimensional abutment-backfill-pile finite element model is created in the OpenSees platform conforming to the geotechnical site conditions at the abutment zone of the Rohtak-Gohana Line Railway Bridge project. Initially, a sample 2D finite element model of the abutment-backfill system is created based on the configuration adopted in the available literature and further validated by comparing the global response of the abutment with the existing one. In the second step, an eigenvalue analysis is performed following the gravity analysis on the main model to get the modal frequencies and modal response in terms of normalized modal vectors. In the third step, monotonic and cyclic pushover analyses are performed on the abutment wall to get a rough estimation of the capacity of the wall against static and cyclic lateral load. In the fourth step, input loadings are chosen that comprise segmental static loads and sinusoidal displacement history. These loadings are applied to the top of the abutment wall laterally for which the research is mainly concerned. A detailed global level behaviour of the system is presented and analyzed hereby explaining the effects of various loading on the overall performance of the abutment-backfill system based on the practically procurable data of the Railway Bridge project mentioned earlier.

## 2 Numerical Simulation of the Abutment Foundation- Backfill system

### 2.1 Brief Description of Rohtak-Gohana Line Railway Bridge Project

The purpose of the project is to raise the Rohtak-Gohana Line in lieu of the Rohtak bypass line to decongest Rohtak city. The bridge site falls under seismic zone- IV which is considered the high-damage risk zone. The railway span lying over the deck is designed for 25T- 2008 standard of axle loading. Since the paper emphasizes only the abutment region of the railway bridge, the detailed structural configuration (Abutment wall, pile cap and piles) and geotechnical data of the soil zone in the proximity to the abutment are of main concern. The type and properties of each soil layer present in the bore log profile up to 30.0 m are mentioned in Table 1.

**Table 1.** Details of the Bore-Log Soil Profile.

Layer no.	Depth range (from ground level) (m)	Span (m)	Soil type	SPT N value	Bulk density (gm/cc)	Friction angle ( $\phi$ ) (degree)
1	0-1.5	1.5	Non-plastic, non-expansive dense compacted silty gravel stratum	38	1.8	26
2	1.5-4.5	3.0	Non-plastic, non-expansive dense compacted silty gravel stratum	60	1.8	26
3	4.5-6.0	1.5	Medium plastic, low expansive & stiff consistency silt and clay with low compressibility	11	1.832	23
4	6.0-18.0	12.0	Non-plastic, non-expansive & medium to dense compacted silty sand	28	1.88	22
5	18.0-19.5	1.5	A medium plastic, low-expansive & very stiff consistency silt and clay with low compressibility	20	1.925	24
6	19.5-30.0	11.5	Non-plastic, non-expansive & dense to very dense compacted silty sand stratum	41	1.925	25

### Validation of Sample Model

In the present context based on the selected literature (Kamalzadeh 2019), a 2D finite element model of the cantilever retaining wall was developed in the OpenSees platform that satisfied the required geometry and characteristics of the wall-foundation-backfill system. The outputs such as wall lateral displacement and horizontal earth pressure profile along the height of the wall at the end of gravity analysis were considered to validate the sample models. Fig. 1a and Fig. 1b display the comparisons of the wall lateral displacement and horizontal earth pressure respectively applicable to Kamalza-deh (2019). It can be observed that the trends in both cases are maintained although some deviation in the soil pressure along the height of the wall is observed. This is possibly due to the lack of proper calibration of the soil constitutive model used in OpenSees and the numerical errors involved in the soil-structure interface zone during the analysis.

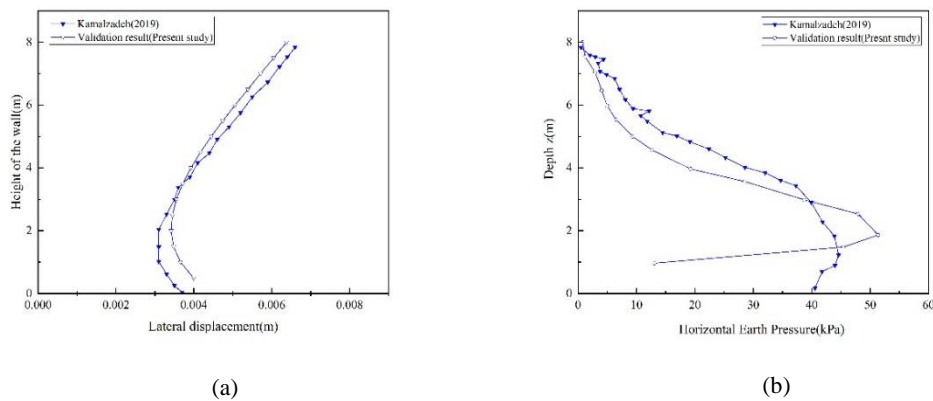
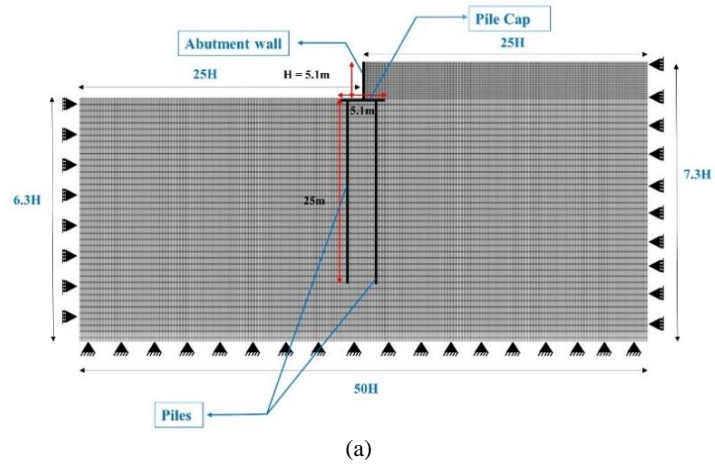


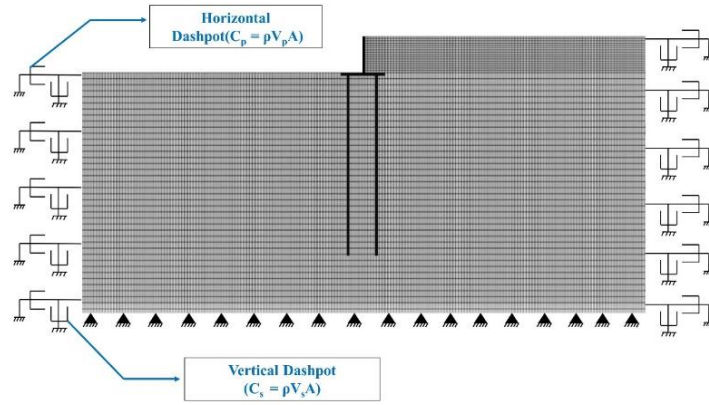
**Fig. 1.** Numerical validation study with Kamalzadeh (2019): (a) Lateral displacement profile (mm); (b) Horizontal earth pressure profile along the height of wall (kPa)

### Description of the main FEM Model

*Selection of Mesh and Domain Size:* Due to sufficient restraint provided by side walls to the backfill soil transversely, the assumption of 2D plane strain is applicable. Besides past researchers (Luco and Hadjian 1974) have checked the utility of representing a 3D linear soil-structure interaction problem by a 2-D plane strain model. The square mesh of 0.3m was assigned to the backfill soil while for the foundation layers, 0.3m by 0.8m mesh size was considered based on the judgement of the depth of layers and keeping in mind the presence of piles. The lateral extent of boundaries is ascertained in the research based on the effect of boundaries on the global response of the structure when subjected to short time impulse loading. In Fig. 2a and Fig. 2b, the schematic representation of the whole numerical domain with specified dimensions is shown for the static and dynamic cases respectively.



(a)



(b)

**Fig. 2.** 2D finite element model: (a) Static case; (b) Dynamic case

*Modelling of Abutment, Pile Cap and Pile.* Abutment wall, pile cap and pile are modelled using elastic beam-column elements having high flexural stiffness due to which the effect of plastic structural deformation can be neglected. During pile-modelling, a concept of equivalency was used as mentioned previously to approximate the 3D behaviour of the pile. The equivalent flexural and axial stiffness of the pile group in a plane strain condition was calculated using the following equations (Prakoso and Kulhawy 2001; Elwakil and Azzam 2016).

$$\text{Equivalent flexural stiffness, } (EI)_{eq} = \left( \frac{n_p \times I_p \times E_p}{L_c} \right) \quad (1)$$

$$\text{Equivalent axial stiffness, } (EA)_{eq} = \left( \frac{n_p \times A_p \times E_p}{L_c} \right) \quad (2)$$

where  $n_p$  is the number of the piles in the out-of-plane direction,  $I_p$  is the moment of inertia of a single pile,  $A_p$  is the cross-sectional area of a single pile and  $L_c$  is the out-of-plane pile cap length. Since the pile and cap elements have the same degrees of freedom per node, simplification was adopted, considering they shared the same node in conjunction without further going into the more complex connection modelling approach.

*Soil-Structure Interface Modelling.* The interaction between the wall-backfill, cap-backfill and cap-foundation soil was modelled by a node-to-node frictional contact element whose formulation is based on Mohr-coulomb law. Since the degrees of freedom are different for the soil and structure, dummy node has to be introduced in order to facilitate the connection. Zero-length contact elements were incorporated to establish the link between the dummy nodes and soil nodes (Kolay et al. 2013). In the case of pile-soil interaction modelling, the zero-length rigid link was placed in between the dummy nodes and the pile nodes ensuring the complete transfer of the displacements between two different bodies while permitting small rotational movements (Sharma et al. 2020).

*Soil Constitutive Model.* The Pressure-Dependent-Multiyield (PDMY02) soil constitutive material (Yang et al. 2003; 2008) was implied to model the constitutive characteristics of the soil layers since the types of the soil in the field fluctuate more or less between the silt, sand and gravel or a combination of them. The formation of yield surface is governed by Drucker-Page model while the plastic deformation follows non-associative flow rule. It considers for the overburden effect ( $K_\sigma$ ) and the effect of previous dilation history on the subsequent contraction phase which adds little modification to existing PDMY model.

*Sequential Analysis.* The total simulation including the analysis part was carried out in a sequential way. In the first stage, after ensuring the proper connection between the structures and soil, the established 2D FEM soil model along with the abutment wall, pile cap and piles was analyzed for gravity load. In this case the side boundaries were kept to move vertical direction only while the base of the model was restricted in the both horizontal and vertical directions. An eigenvalue analysis was performed subsequently after the gravity analysis to get the idea of structural mode shapes. In the third step two distinct types of pushover analysis such as static and cyclic pushover were carried out. Under the static condition, the static monotonic pushover was performed to get the idea of the magnitude of the yield lateral capacity and corresponding displacement. In the final stage, input loads were selected based on the pushover results which were applied at the top of the abutment wall. For static case, the boundary conditions were kept as at the time of gravity analysis while for dynamic case, both horizontal and vertical L-K dashpots were attached at the side boundaries assuming the bottom of the domain as rigid rock.

*Details of Lateral Loadings.* The yield lateral load capacity is denoted hereby as  $q_u$ , obtained from the static monotonic pushover curve using the double tangent method. For the static case, the behaviour under a set of loading i.e.  $0.2q_u$ ,  $0.4q_u$ ,  $0.6q_u$ ,  $0.8q_u$ ,  $1.0q_u$  and  $1.2q_u$  was considered which were acting towards the passive direction of the abutment wall-backfill system. Analysis was performed under each load individually. For the dynamic loading case, the yield displacement was chosen as the amplitude of the sinusoidal displacement history and the frequency of the motion was considered as the 1<sup>st</sup> modal frequency obtained from the eigenvalue analysis presuming it to be the most dominant modes of vibration. The duration of the sinusoidal loading was taken 3 seconds mainly keeping in mind the time elapsed during analysis in the presence of nonlinearity and the number of simulation runs.

### 3 Results and Discussions

*Outcomes of Eigenvalue Analysis.* The 1<sup>st</sup> modal frequency is found to be 1.44 Hz. The mode shape of the corresponding frequency for the abutment wall is shown in Fig. 3 where normalized eigenvectors are defined as the ratio of eigenvectors to the magnitude of the maximum one.

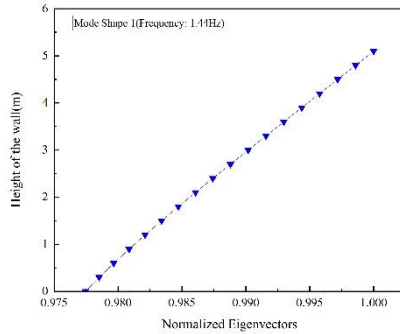


**Fig. 3.** Lateral mode shape of the abutment wall for 1<sup>st</sup> fundamental frequency

*Outputs of Pushover Analysis.* From the monotonic pushover curve Fig. 4a, the yield lateral capacity ( $q_u$ ) is approximately found to be 2250 kN, and the corresponding value of the lateral displacement is around 0.07m. From the cyclic pushover curves shown in Fig. 4b, the yield capacity was determined as 2000 kN corresponds to 0.10m lateral displacement for a positive peak amplitude cycle case.

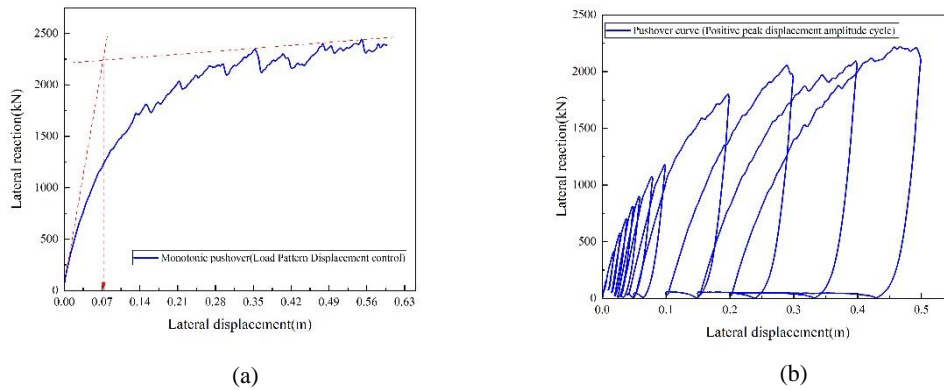


**Fig.4.** Pushover curves: (a) Monotonic; (b) Positive peak amplitude cycle

*Response to Static Loading.* The global responses centered to only abutment-backfill system are presented in the context without considering pile cap and pile behaviour. All the absolute maximum global outputs for the different magnitudes of static loading are presented in Table 2 for the sake of comparison. The lateral displacement profile along

the height of the abutment wall for low to high static loads is shown in Fig. 5a. For low load  $0.2q_u$ , a combination of passive and active deflection is observed where the active zone is created at the base of the wall. But with the increment in load, the wall is totally moved towards the backfill with maximum displacement at the top as expectable. Also, it is observed that with the increment in the load, the displacement at the top and base differs significantly from each other. It may be due to the plastic zone formation in the soil behind the top of the wall while at the base the movement is getting restricted by the pile cap. The cumulative reaction along the height of the wall follows the same trend for all loads with a maximum at the base shown in Fig. 5b. The lateral stress distribution behind the wall shown in Fig. 5c follows a similar nonlinear trend for all load cases exhibiting high lateral stress at the zone close to the application of load. The wall shear force and bending show a similar pattern for all load cases where the shear force is attaining maximum value at the top of the wall due to an unbalanced external force being applied at that point. The bending moment approaches zero at the top and highest at the base of the wall which is supposed to occur. Due to the high bending moment at the base, the critical zone is supposed to be concentrated on that specific region of the stem wall from the structural failure aspect. Although in the present study, structural failure is not considered due to the assumption of the elastic and high bending stiffness of the structure. The shear force and bending moment diagrams for the wall are represented in Fig. 5d and 5e respectively for low to high values of the static lateral load.

**Table 2.** Absolute Maximum Global Outputs for Static Loading.

Substructures	Global Outputs(Unit)	Static Load (kN)					
		$0.2q_u$	$0.4q_u$	$0.6q_u$	$0.8q_u$	$q_u$	$1.2q_u$
Abutment Wall	Lateral Displacement (mm)	6.47	19.82	35.98	55.35	78.67	105.58
	Cumulative Base Reaction(kN)	377.38	658.86	944.38	1230.48	1509.38	1764.47
	Shear Force(kN)	439.80	880.71	1318.02	1757.89	2217.46	2666.56
	Bending Moment(kN-m)	1326.15	2768.48	4196.09	5641.17	7168.05	8747.87



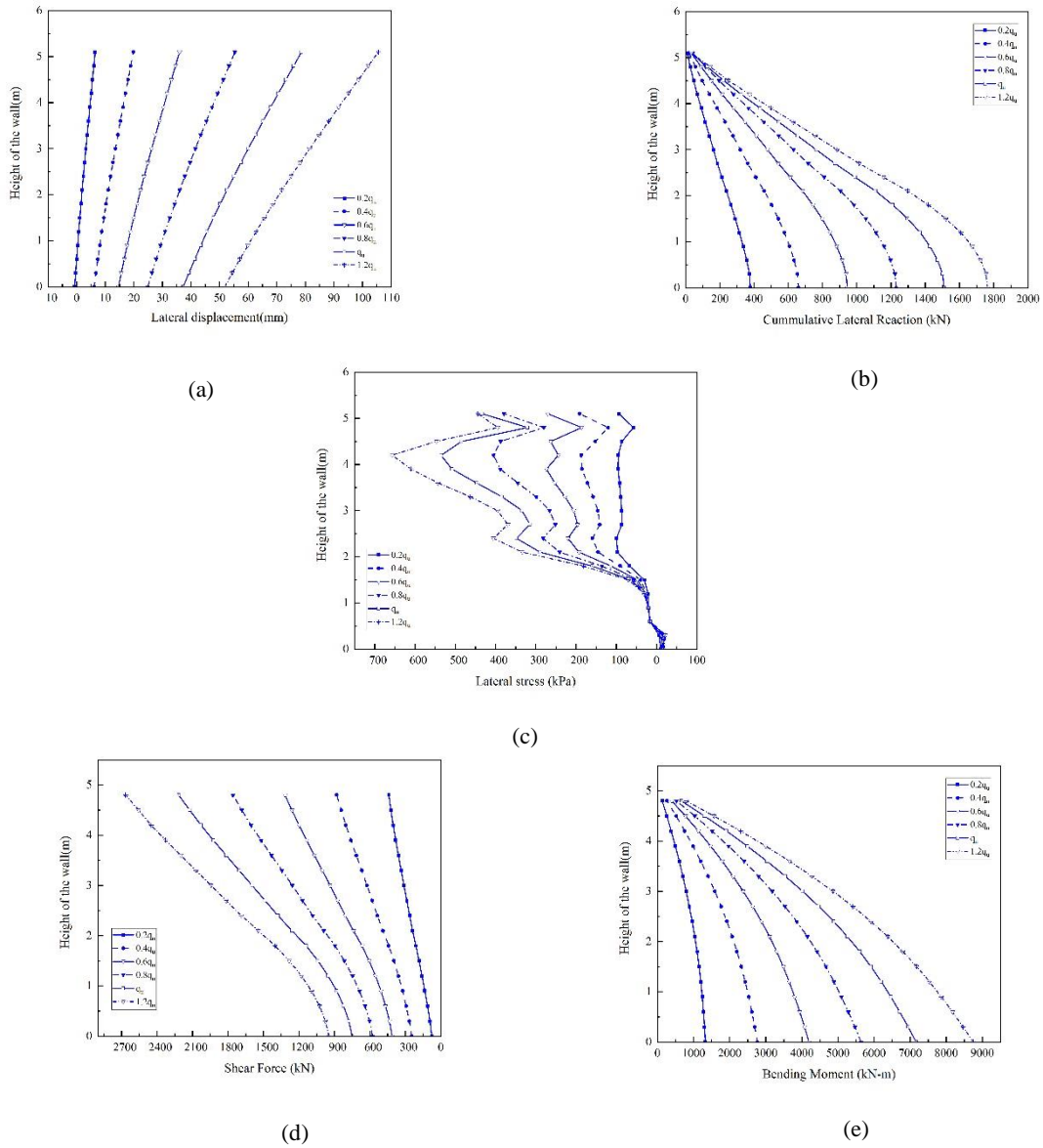


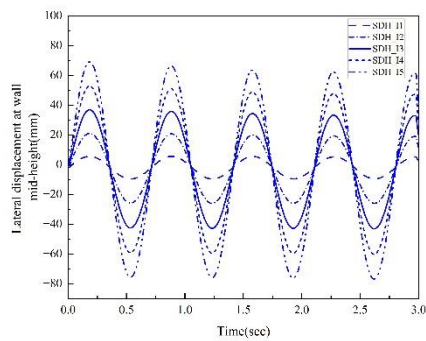
**Fig.5.** Global outputs for different magnitudes of static loading: (a) Lateral displacement; (b) Cumulative lateral reaction; (c) Lateral stress; (d) Shear force; (e) Bending moment

*Response to Dynamic Loading.* To identify the combinations of the input motion, a nomenclature pattern is adopted and followed throughout the discussion shown in Table 3. The effect of amplitude of the motion are elaborately studied by comparing responses in terms of the absolute maximum global outputs of the substructures. In Fig. 6a, it can be observed that for 1<sup>st</sup> mode, with the increase in amplitude, the lateral displacement history recorded at mid-height of the abutment wall achieves a higher peak envelope. Besides the maximum absolute lateral displacement profile along the height of wall shown in Fig. 6b reflects the increase in the top displacement value with the increment in amplitude. Although the trend follows the 1<sup>st</sup> mode shape, the relative deformation along the wall differs a lot for high amplitude. The change in the cumulative base reactions shown in Fig. 6c follows the same fashion as the lateral displacement with increasing amplitude. The variation in maximum shear force and bending moment with amplitudes are shown in Fig. 6d and 6e respectively. The maximum shear force occurs at top of the abutment wall in all cases due to the presence of unbalanced loads while

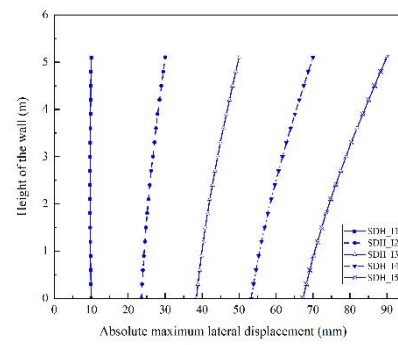
the maximum bending moment takes place at the base as expected. With an increment in amplitude, they both increase simultaneously. For comparison purpose, the entire results for 1<sup>st</sup> mode are mentioned in Table 4 for different amplitudes.

**Table 3.** Nomenclatures of input sinusoidal displacement history.

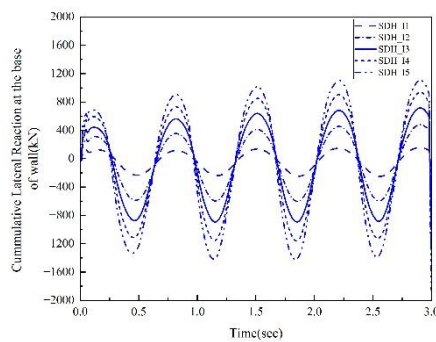
Mode	Frequency (Hz)	Amplitude (m)	Designation
I	1.44	0.01	SDH_I1
		0.03	SDH_I2
		0.05	SDH_I3
		0.07	SDH_I4
		0.09	SDH_I5



(a)



(b)



(c)

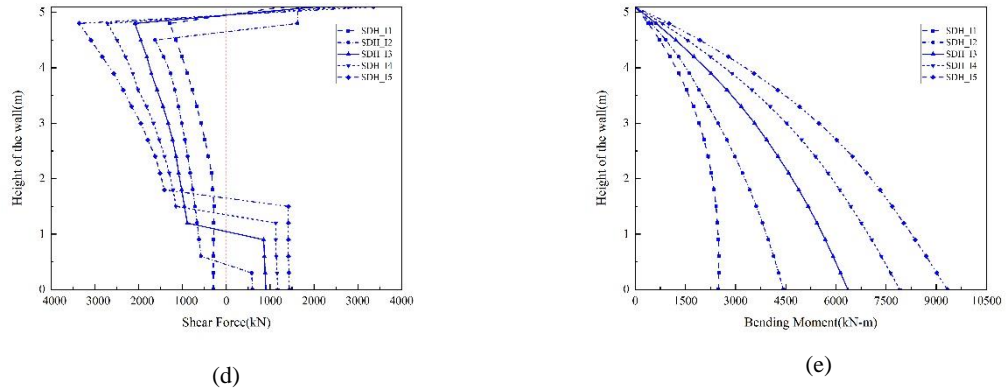


**Fig.6.** Global outputs for different amplitudes of dynamic loading: (a) Lateral displacement history at the mid-height of wall; (b) Absolute maximum lateral displacement; (c) Cumulative lateral reaction at the base; (d) Shear force; (e) Bending moment

**Table 4.** Comparison chart for absolute maximum global Outputs considering dynamic loading (Mode-I).

Substructures	Global Outputs(Unit)	Amplitude(m)				
		0.01	0.03	0.05	0.07	0.09
Abutment Wall	Lateral Displacement at mid-height (mm)	9.64	26.05	43.16	60.26	76.95
	Cumulative Base Reaction(kN)	251.16	602.60	926.44	1378.60	1866.14
	Shear Force(kN)	1289.2	1625.86	2085.75	2711.15	3358.52
	Bending Moment(kN-m)	2497.61	4433.84	6354.57	7912.96	9329.41

## 4 Summary and Conclusions

The paper illuminates the need to study the effect of static and dynamic lateral loading on the response of the abutment-backfill system. A few conclusions can be drawn from this study that is mentioned hereby as follow:

(i) Pushover analysis shows different yield capacities of the abutment-backfill system depending upon the load applied to the structure. Higher yield capacity is observed in static monotonic pushover case compared to cyclic pushover analysis as expected due to degradation.

(ii) Eigenvalue analysis shows the less variation in relative deformation along the height of wall at 1<sup>st</sup> fundamental frequency.

(iii) For the static load case, the global responses of the abutment wall are found to rely upon several factors such as the spreading of the plastic zone at the backfill region, the load application point and the amount of unbalanced load.

(iv) The influence of different amplitude of displacement history corresponding to specific mode of vibration are detectable. With increase in amplitude, the effect of modal shape on the relative deformation gets reduced.

## References

1. Argyroudis, A., Kaynia, M.A. and Pitilakis, K.: Development of fragility functions for geotechnical constructions: Application to cantilever retaining walls. *Soil Dynamics and Earthquake Engineering*, 50:106-116 (2013).
2. Argyroudis, A.S., Mitoulis, A.S. and Pitilakis D.K.: Seismic response of bridge abutments on surface foundation subjected to collision forces. 4th International Conference on Computational Methods in Structural Dynamics and Earthquake Engineering, Proceedings - An IACM Special Interest Conference, pp.860-878 (2013).
3. Dicleli, M.: Integral abutment-backfill behavior on sand soil-pushover analysis approach. *Journal of Bridge Engineering*, 10(3): 354-364 (2005).
4. Ellis, A.E. and Springman, M.S.: Modelling of soil-structure interaction for a piled bridge abutment in plane strain FEM analyses. *Computer and Geotechnics*, 28:79-98 (2001).
5. Elwakil, Z.A. and Azzam, R.W.: Experimental and numerical study of piled raft system. *Aleandria Engineering Journal*, 55:547-560 (2016).
6. Kamalzadeh, A. and Pender, J.M.: Numerical investigation of gravity retaining wall foundation failure mechanisms. Pacific Conference on Earthquake Engineering, Auckland, New Zealand (2019).
7. Kolay, C., Prashant, A. and Jain, K.S.: Nonlinear dynamic analysis and seismic coefficient for abutments and retaining walls. *Earthquake Spectra*, Vol. 29, No. 2, 427-451 (2013).
8. Lemnitzer, A., Ahlberg, E.R., Nigbor, R.L., Shamsabadi, A., Wallace, J.W., and Stewart, J.P.: Lateral performance of full-scale bridge abutment wall with granular backfill. *Journal of Geotechnical and Geoenvironmental Engineering*, 135(4): 506-514 (2009).
9. Luco, E.J. and Hadijian H.A.: Two-dimensional approximations of the three-dimensional soil-structure interaction problem. *Nuclear Engineering and Design*, 31:295-203 (1974).
10. Prakoso, A.W. and Kulhawy, H.F.: Contribution to piled raft foundation design. *Journal of Geotechnical and Geoenvironmental Engineering*, Vol. 127, No. 1 (2001).
11. Sharma, N., Dasgupta, K. and Dey, A.: Natural period of reinforced concrete building frames on pile foundation considering seismic soil-structure interaction effects. *Structures*, 27:1594-1612 (2020).
12. Stewart, J.P., Taciroglu, E., and Wallace, J.W.: Full scale cyclic testing of foundation support systems for highway bridges. Part II: abutment backwalls. Department of Civil and Environmental Engineering University of California, Los Angeles (2007).
13. Wilson, P., and Elgamal, A.: Large-scale passive earth pressure load-displacement tests and numerical simulation. *Journal of Geotechnical and Geoenvironmental Engineering*, 136(12): 1634-1643 (2010).
14. Yang, Z., Elgamal, A., and Parra, E.: Computational model for cyclic mobility and associated shear deformation. *Journal of Geotechnical and Geoenvironmental Engineering*, 129 (11): 1119-1127 (2003).
15. Yang, Z., Lu, J., and Elgamal, A.: OpenSees soil models and solid fluid fully coupled elements: User's manual. San Diego: Department of Structural Engineering, University of California (2008).